

Estimation of Stopped Protons at RHIC BES Energies

Dhananjaya Thakur,¹ Sunil Jakhar,¹ Prakhar Garg,^{1,*} and Raghunath Sahoo^{1,†}

¹*Discipline of Physics, School of Basic Sciences,
Indian Institute of Technology Indore, Indore- 453552, INDIA*

(Dated: November 17, 2016)

The recent net-proton fluctuation results of the STAR experiment from beam energy scan (BES) program at RHIC have drawn much attention to explore the QCD critical point and the nature of deconfinement phase transition. There have been many speculations that the non-monotonic behaviour around 19.6 GeV in STAR results may be due to the existence of QCD critical point. However, the experimentally measured proton distributions contain protons from heavy resonance decays, from baryon stopping and from the production processes. Further, these proton distributions are used to estimate the net-proton number fluctuations as it is difficult to disentangle the protons from the above sources. Assuming that any criticality in the system could affect the particle production, in order to study the dynamical fluctuations at different center of mass energies, it will be interesting to devise a method which accounts for the produced baryons i.e. the protons here. In the present work we present a method to estimate the number of stopped protons at RHIC BES energies for central 0% – 5% Au+Au collisions within STAR acceptance and discuss its implications on the net-proton fluctuation results.

PACS numbers: 25.75.Dw, 25.75.Nq, 12.38.Mh

I. INTRODUCTION

One of the main motivations of heavy ion collisions is to explore the QCD phase diagram of strong interaction. Quantum chromodynamics (QCD) predicts a phase transition from a hadron gas (HG) phase to a quark gluon plasma (QGP) phase by varying the temperature (T) and/or baryon density (μ_B) of the system. Lattice QCD calculations indicate a smooth crossover along the temperature axis, while various other models predict a first order phase transition at high baryon density. The existence of the QCD critical point is thus expected as the first order phase transition line should end somewhere at finite μ_B and T [1–8]. This is also one of the main motivations behind the recent STAR net-proton [9], net-charge [10] and PHENIX net-charge [11] measurements. It is necessary to look into the dynamical behaviour of the produced system by considering the effects of baryon stopping and initial state participant fluctuations, and their observable effects. In order to do this, the present work is an effort to quantify the effect of stopped baryons, which are prevalent at lower collision energies around the RHIC BES, where a possible critical point in the QCD phase diagram is expected to be observed.

The phenomenon of baryon stopping could be used as a direct tool to explore the QCD phase transition and as a probe of equation of state (EoS) of the system [12]. The

mid-rapidity reduced curvature from the net-proton rapidity distribution is used as an observable of the baryon stopping. As discussed in Ref.[12], the behaviour of the mid-rapidity curvature with $\sqrt{s_{NN}}$ has been studied and a zig-zag type of structure is observed. A three-fluid dynamics (3FD) calculation with hadronic EoS fails to explain the observed structure, whereas 3FD with first order phase transition from a hadronic phase to a deconfined phase of quark-gluon plasma qualitatively reproduces the structure [12]. Hence, it is argued that the non-monotonous behaviour of the baryon stopping is due to phase transition and is most probably first order in nature. Theoretical studies based on STAR net-proton fluctuation [9] hints for a phase transition at low $\sqrt{s_{NN}}$ taking inclusive protons i.e. from both production and stopping. However, as baryon stopping plays a major role at lower collision energies and almost vanishes at higher energies, there seems to be a need to disentangle the contribution of stopped baryons and the produced baryons in order to understand the observed structure and hence the QCD phase diagram.

The present work is motivated by the fact that to look for the fluctuations of dynamical origin to search for a critical point one should look for the net-baryon number fluctuations because of production mechanism. But, most of the experimentally measured proton distributions contain the protons from stopping and resonance decays besides from the production. Also, it has been studied earlier that the change in the mean of proton distributions (which will be there after subtracting the stopped protons) will have large effect on the correlation of the protons and antiprotons and it can influence the higher moments of net-protons fluctuations [13]. Particularly, at lower center of mass energies the stopping contribution is most dominant and it will be interesting to look for the dynamical fluctuations after removing these

*Present Address: Department of Physics and Astronomy, Stony Brook University, SUNY, Stony Brook, NY 11794-3800, USA

†Electronic address: Corresponding Author Email: Raghunath.Sahoo@cern.ch

stopped protons. Although, various other effects on the conserved number fluctuations have been studied earlier in Refs. [13–18].

Further, In heavy ion collision experiments, a part of the incident energy of the two colliding nuclei is used for fireball production and hence the formation of secondary particles. Therefore, the formation of the QGP in relativistic heavy ion collisions depends on the amount of stopping between the colliding ions particularly at low center of mass energies. Therefore baryon stopping is an important tool to understand the particle production mechanism. As the net baryon number is conserved and rapidity distribution is modified due to re-scattering of the particles after the collision, the net baryon rapidity distribution hence becomes a good probe to give information about the baryon transport and baryon stopping. Since, the neutrons are not measured mostly in heavy ion experiments, the net-proton rapidity distributions are used to quantify the baryon stopping [19–24].

In the present work we use the data of net proton rapidity distributions for most central Au+Au collisions measured at AGS, SPS and BRAHMS at RHIC. Further, we use a two source function [12], to analyze the net-proton distributions at different center of mass energies. It is a combination of two thermal sources with a shift in their rapidities. The same two source function is used in the present work to calculate the percentage of stopped protons. Afterwards, the percentage of stopped protons with $\sqrt{s_{NN}}$ is parametrized and the values at RHIC BES energies are interpolated. Finally, we estimate the contribution of stopped protons in rapidity $|y| < 0.5$ and transverse momentum between $0.4 \text{ GeV}/c < p_T < 0.8 \text{ GeV}/c$, which is used to measure the protons and anti-protons by STAR experiment for net-proton fluctuation studies [9].

The paper is organized as follows. In the following section we discuss the method used for the present analysis. It is divided into three sub-sections: (a) Estimation of baryon stopping in $|y| < 0.5$, (b) Estimation of stopped protons in STAR transverse momentum (p_T) range, (c) Contribution of stopped protons in STAR measurements. Finally in Section III, we summarize our work and discuss the implications of this work to the net-proton fluctuation results of STAR experiment at RHIC.

II. METHOD

A. Estimation of baryon stopping in $|y| < 0.5$

Net-proton rapidity distribution of the experimental data is best described by the following function as is proposed in Ref. [12].

$$\frac{dN}{dy} = a \left[\exp\left\{-\frac{1}{w_s} \cosh(y - y_{cm} - y_s)\right\} + \exp\left\{-\frac{1}{w_s} \cosh(y - y_{cm} + y_s)\right\} \right] \quad (1)$$

where a , y_s and w_s are the fit parameters of the function and y_{cm} is the center of mass rapidity of the colliding

nuclei. Eq.1 is the sum of two thermal sources shifted by rapidity $\pm y_s$ from the mid-rapidity. w_s is the width of the sources and is given by $w_s = (\text{temperature})/(\text{transverse mass})$, with the assumption that there is no spread of collective velocities in the sources with respect to source rapidities. Here we are concerned about symmetric collisions, hence parameters of the two sources are identical. Parameters y_s and w_s are calculated from the fit of the function to the rapidity distribution of secondary particles. We have used Eq. 1 to fit the net-proton rapidity distributions to quantify the baryon stopping.

Baryon stopping is directly measured via the rapidity distribution of net-protons (i.e. the number of protons minus antiprotons). At low energies like at AGS, the production of antiprotons is very small so the net-proton distribution is same as the proton distribution and the rapidity distribution is peaked at mid-rapidity [12]. As the collision energy increases a dip begins to appear at mid-rapidity ($y \approx 0$) and the peak shifts toward the forward and backward rapidities, due to the production of antiprotons at mid rapidity. This indicates that with increase of energy the transparency at the mid rapidity increases. The rapidity loss of the particle is defined as $y_{loss} = y_b - y$, where $y_b = \log(\sqrt{s_{NN}}/m_p)$ is the beam rapidity with m_p being the mass of proton.

Therefore, the net-baryon number at mid rapidity is the measure of baryon stopping [19–21]. To estimate the quantity of stopping we have used Eq. 1 to fit the data of rapidity distribution for most central Au+Au collisions at AGS (2, 4, 8 AGeV), and BRAHMS at RHIC (62.4 and 200 GeV). The fitting is performed using TMinute class available in ROOT library with χ^2 minimization. Fig. 1 shows the fit functions for different energies. Further, these fit functions are used to estimate the baryon stopping at corresponding collision energy.

In the center of mass system, the maximum rapidity that a outgoing particle can have after the collision is y_b which is only possible for full transparency. Therefore by using Eq. 1, the fraction of stopped protons in $|y| < 0.5$ at a particular energy can be calculated as:

$$f_{stopped}^{proton} = \frac{\int_{-0.5}^{0.5} \frac{dN}{dy} dy}{\int_{-y_b}^{y_b} \frac{dN}{dy} dy} \quad (2)$$

Hence, the percentage of stopped protons can be estimated as:

$$N_{stopped}^{proton} = f_{stopped}^{proton} \times 100 \%. \quad (3)$$

It should be noted here that $\int_{-y_b}^{y_b} \frac{dN}{dy} dy$ gives the total number of participating protons (N_{part}^B) and for top central Au+Au collisions, $N_{part}^B \approx 158$. The calculated percentage of stopped protons at these energies are shown in TABLE. I.

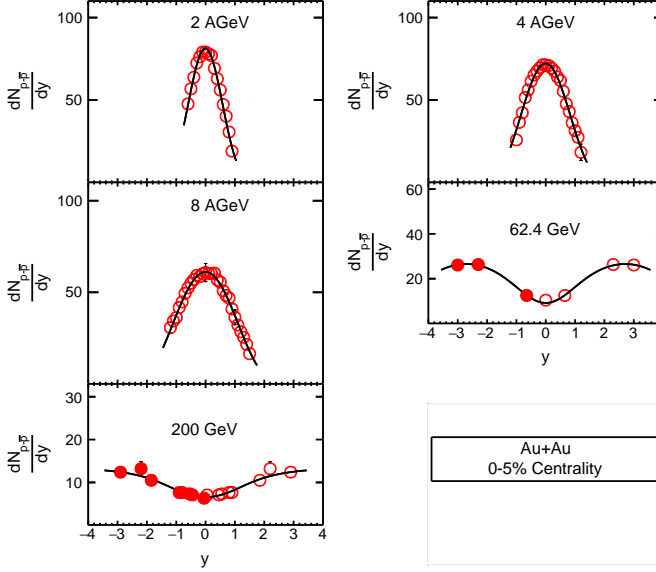


FIG. 1: The rapidity densities of protons at 2, 4, 8 AGeV (AGS) and net-proton ($N_p - N_{\bar{p}}$) (for RHIC energies) from central Au+Au collisions at AGS and RHIC in center-of-mass system. Experimental data are from E802 [25], E877 [26], E917 [27], E866 [28] and RHIC experiments [20, 24]. The open circles are experimentally measured data points and the filled circles are the mirror reflections, assuming a symmetry in particle production. Solid lines represent the two source fit function given by Eq.1.

TABLE I: Fraction of stopped protons in $|y| < 0.5$ at different energies

$\sqrt{s_{NN}}$	$N_{\text{stopped}}^{\text{proton}} [\%]$
2 AGeV	64.22 ± 0.10
4 AGeV	52.16 ± 0.15
6 AGeV	47.59 ± 0.12
8 AGeV	44.61 ± 0.12
62.4 GeV	4.57 ± 0.10
200 GeV	2.91 ± 0.0

Thereafter, by converting the lab energy to center of mass energy, a study of stopped protons with $\sqrt{s_{NN}}$ is done. The decreasing behaviour of stopped protons ($N_{\text{stopped}}^{\text{proton}}$) with $\sqrt{s_{NN}}$ is best described by an exponential function as is shown in FIG. 2. Our observations go inline with the earlier study [19]. Hence a parametric form of the stopped protons with $\sqrt{s_{NN}}$ is obtained. Using this parametric function, we have interpolated the percentage of stopping at RHIC BES energies within $|y| < 0.5$ for $\sqrt{s_{NN}} = 7.7, 11.5, 19.6, 27, 39, 62.4$ and 200 GeV. The values are tabulated in TABLE II.

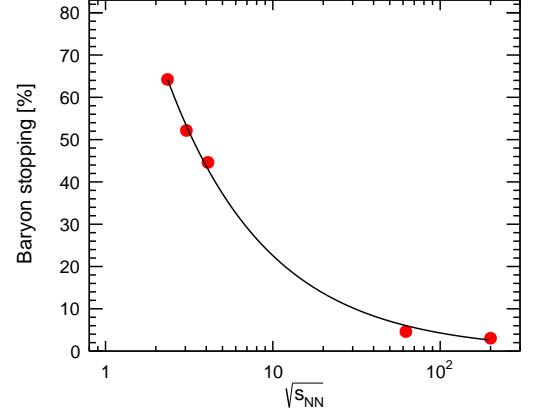


FIG. 2: Percentage of baryon stopping as a function of $\sqrt{s_{NN}}$, fitted with an exponentially decreasing function with energy.

TABLE II: Percentage of stopped protons at different RHIC BES energies in $|y| < 0.5$:

$\sqrt{s_{NN}}$ [GeV]	7.7	11.5	19.6	27	39	62.4	200
$N_{\text{stop}}^p [\%]$	27.27	20.43	13.90	11.03	8.46	6.03	2.60
Error{ $N_{\text{stop}}^p [\%]$ }	1.30	1.34	1.25	1.15	1.03	0.86	0.51

B. Estimation of stopped protons in STAR p_T acceptance

In the previous section we have estimated percentage of stopped protons in $|y| < 0.5$ at BES energies. But, the STAR experiment has measured the protons and antiprotons in $0.4 \text{ GeV}/c < p_T < 0.8 \text{ GeV}/c$ and the higher order cumulants of net-proton distributions are measured in this acceptance [9]. In the previous section we have already estimated the baryon stopping in mid rapidity region, now we also calculate it in the STAR p_T acceptance. Here we assume that the stopped protons are uniformly distributed over the whole p_T -range. To estimate the fraction of the stopped protons in STAR p_T acceptance we have fitted the protons p_T spectra at different available BES energies. The fitting is performed with a Levy-Tsallis function which is given by Eq.11 of Ref. [33] for $\sqrt{s_{NN}} = 9.2 \text{ GeV}$, 62.4 GeV and 200 GeV. Similarly, for $\sqrt{s_{NN}} = 19.6 \text{ GeV}$, the fitting function as is given by Eq.6 in Ref. [29] is used. The fitting results of STAR proton data are shown in FIG. 3. We integrate the fitted functions in a particular energy from $p_T = 0.0$ to $p_T = \infty$ and $p_T = 0.4$ to $0.8 \text{ (GeV}/c)$. Thus the total number of protons in the whole p_T range and the number of protons in $0.4 \text{ GeV}/c < p_T < 0.8 \text{ GeV}/c$ are calculated.

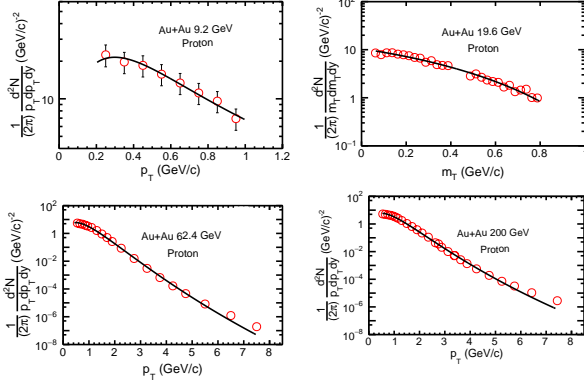


FIG. 3: Invariant yield of protons at $\sqrt{s_{NN}} = 9.2$ GeV [35], 19.6 GeV [30], 62.4 GeV [31], 200 GeV [32] for most central Au + Au collisions. The scattered open circles are the experimental data measured by the STAR Collaboration. The solid lines are the fitting with Levy-Tsallis [33] for $\sqrt{s_{NN}} = 9.2$ GeV, 62.4 GeV, 200 GeV and Tsallis function [29] for $\sqrt{s_{NN}} = 19.6$ GeV.

Then the fraction of protons falling in $0.4 \text{ GeV}/c < p_T < 0.8 \text{ GeV}/c$ region is estimated as,

$$f_{p_T}^{protons} = \frac{N_{p_T}^{protons}(0.4 < p_T < 0.8)}{N_{p_T}^{protons}(full \ p_T)} \quad (4)$$

Hence the percentage of protons in STAR p_T range is given by

$$N_{p_T}^{proton} = f_{p_T}^{protons} \times 100\% \quad (5)$$

This gives the fraction of stopped protons contributing in STAR p_T acceptance. To calculate the percentages in the BES energies, we have parametrized these numbers with $\sqrt{s_{NN}}$ by first order polynomial as is shown in FIG. 4. Then the contributions at different BES energies are interpolated. The extracted values are tabulated in TABLE III. It is clear from the table that the fraction of stopped protons decrease with collision energy.

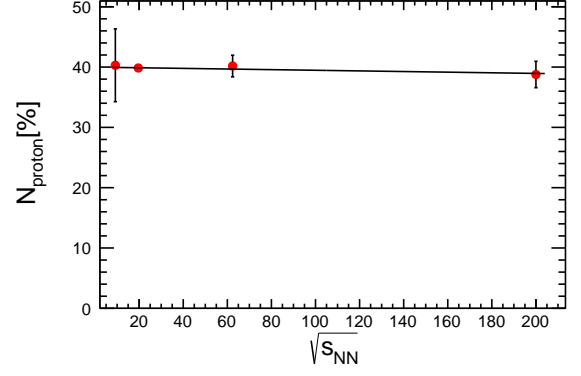


FIG. 4: Percentage of protons in $0.4 \text{ GeV}/c < p_T < 0.8 \text{ GeV}/c$ as a function of $\sqrt{s_{NN}}$, being well described by a first order polynomial.

TABLE III: Percentage of protons obtained from p_T spectra at different STAR BES energies:

$\sqrt{s_{NN}}[\text{GeV}]$	7.7	11.5	19.6	27	39	62.4	200
$N_{p_T}^p \%$	39.95	39.93	39.88	39.84	39.79	39.66	38.94
Error $\{N_{p_T}^p \%\}$	0.60	0.58	0.54	0.52	0.52	0.63	2.11

C. Contribution of stopped protons in STAR measurements

In top central Au+Au collisions, there are around 158 protons participating in a collision. We have already estimated the number of protons in TABLE. I for $|y| < 0.5$ and in TABLE. III for $0.4 \text{ GeV}/c < p_T < 0.8 \text{ GeV}/c$. Therefore, one can easily calculate the effect of both to estimate the total stopped protons in STAR acceptance as:

$$N_{stopped}^{proton}(STAR) = 158 \times N_{stopped}^{proton} \% \times N_{p_T}^{proton} \% \quad (6)$$

where $N_{stopped}^{proton}(STAR)$ is the total contribution of stopped protons in STAR acceptance. In TABLE. IV we summarize the total stopped protons at BES energies in STAR acceptance.

TABLE IV: Number of stopped protons at different RHIC BES energies in STAR acceptance:

$\sqrt{s_{NN}} [\text{GeV}]$	7.7	11.5	19.6	27	39	62.4	200
N_{stop}^{proton}	17.21	12.89	8.76	6.94	5.32	3.78	1.6
Error $\{N_{stop}^{proton}\}$	0.86	0.86	0.80	0.73	0.65	0.54	0.33

FIG. 5 shows the energy dependent behaviour of the stopped protons, which is consistent with the fact that stopping is more at lower energies as compared to the higher energies.

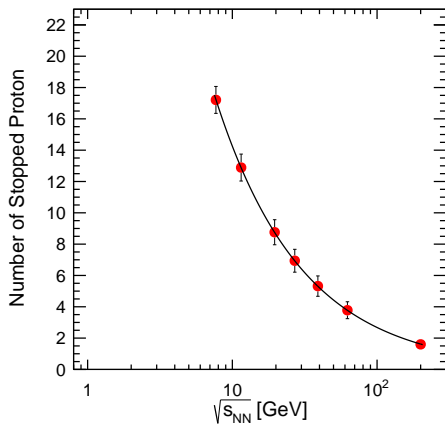


FIG. 5: Mean number of protons from baryon stopping in STAR acceptance as a function of $\sqrt{s_{NN}}$, showing an exponential decrease with energy.

It is interesting to note that after subtracting the stopped protons from the mean of STAR proton distributions [9], the remaining produced protons are consistent with the antiprotons measured by the STAR experiment. This can be seen from Table. V. There is a small discrepancy in between these two numbers for 7.7 GeV and 11.5 GeV measurements. This may be due to larger uncertainties in the experimental measurements of protons itself.

TABLE V: Column wise (a) $\sqrt{s_{NN}}$ at which the analysis is performed (b) Mean number of protons obtained from baryon stopping in STAR acceptance [$N_{\text{stopped}}^{\text{proton}}(\text{STAR})$] (c) Mean number of protons measured by STAR experiment [$N_{\text{STAR}}^{\text{proton}}$] [34] (d) Diff. = [$N_{\text{STAR}}^{\text{proton}} - N_{\text{stopped}}^{\text{proton}}(\text{STAR})$] (e) Mean number of antiprotons measured by STAR experiment [$N_{\text{STAR}}^{\text{antiproton}}$]

(a)	(b)	(c)	(d)	(e)
$\sqrt{s_{NN}}$	$N_{\text{stopped}}^{\text{proton}}(\text{STAR})$	$N_{\text{STAR}}^{\text{proton}}$	Diff.	$N_{\text{STAR}}^{\text{antiproton}}$
7.7	17.21 ± 0.86	18.92 ± 0.01	1.71 ± 0.86	0.165
11.5	12.89 ± 0.86	15.00 ± 0.01	2.10 ± 0.86	0.49
19.6	9.73 ± 0.80	11.37 ± 0.00	1.63 ± 0.80	1.15
27.0	7.61 ± 0.73	9.39 ± 0.00	1.78 ± 0.73	1.65
39.0	5.78 ± 0.65	8.22 ± 0.00	2.44 ± 0.65	2.38
62.4	3.78 ± 0.54	7.25 ± 0.00	3.47 ± 0.54	3.14
200	1.54 ± 0.33	5.664 ± 0.00	4.12 ± 0.33	4.11

III. SUMMARY

In the present work we use the data of net proton rapidity distributions for most central Au+Au collisions

measured by different experiments. Further, we use a two source function [12], to analyze the net-proton distributions and the percentage of stopped protons at different center of mass energies. Then the percentage of stopped protons is interpolated at RHIC BES energies. Afterwards, using invariant transverse momentum spectrum we have estimated the fraction of the number of protons contributing to STAR acceptance. Finally, using these two numbers, we estimate the contribution of stopped protons in rapidity $|y| < 0.5$ and transverse momentum between $0.4 \text{ GeV}/c < p_T < 0.8 \text{ GeV}/c$, which is used to measure the protons and anti-protons by STAR experiment for net-proton fluctuation studies [9].

The measurements of net-proton higher order cumulants are done by STAR experiment [9] at mid rapidity ($|y| < 0.5$) within $0.4 \text{ GeV}/c < p_T < 0.8 \text{ GeV}/c$ for most central Au+Au collisions in a wide range of $\sqrt{s_{NN}}$ to explore the QCD phase diagram and to locate the critical point. For this analysis the measured protons include the stopped protons, protons coming from resonances and the produced protons. The critical point of QCD phase diagram is expected to show large dynamical fluctuations in the produced conserved charges. Therefore, it will be exciting to see these results after removing the contribution of stopped protons which have significant contribution particularly at lower collision energies. In the present work we have presented a method to estimate the number of stopped protons in STAR acceptance at all the RHIC BES energies. We reserve the problem for future, to estimate higher order cumulants of net-proton distributions after removing the stopped protons from STAR measurements.

IV. ACKNOWLEDGEMENT

Dhananjaya Thakur acknowledges the financial support from University Grants Commission, New Delhi of Government of India. The authors would like to gratefully acknowledge discussions with Dr. Dipak K. Mishra. SJ acknowledges the Masters Program of IIT Indore, which has given an exposure to research environment in the ALICE group and as an outcome of which this paper is a witness.

[1] M. A. Stephanov, K. Rajagopal and E. V. Shuryak, Phys. Rev. Lett. **81**, 4816 (1998).

[2] M. G. Alford, K. Rajagopal and F. Wilczek, Phys. Lett. B **422**, 247 (1998).

- [3] M. A. Stephanov, Phys. Rev. Lett. **76**, 4472 (1996).
- [4] Y. Aoki, G. Endrodi, Z. Fodor, S. D. Katz and K. K. Szabo, Nature **443**, 675 (2006).
- [5] K. Fukushima and T. Hatsuda, Rept. Prog. Phys. **74**, 014001 (2011).
- [6] M. A. Stephanov, Prog. Theor. Phys. Suppl. **153**, 139 (2004), Int. J. Mod. Phys. A **20**, 4387 (2005).
- [7] Z. Fodor and S. D. Katz, JHEP **0404**, 050 (2004).
- [8] M. A. Stephanov, K. Rajagopal and E. V. Shuryak, Phys. Rev. D **60**, 114028 (1999).
- [9] L. Adamczyk *et al.* [STAR Collaboration], Phys. Rev. Lett. **112**, 032302 (2014).
- [10] L. Adamczyk *et al.* [STAR Collaboration], Phys. Rev. Lett. **113**, 092301 (2014).
- [11] A. Adare *et al.* [PHENIX Collaboration], Phys. Rev. C **93**, 011901 (2016).
- [12] Y. B. Ivanov, Phys. Lett. B **690**, 358 (2010).
- [13] D. K. Mishra, P. Garg and P. K. Netrakanti, Phys. Rev. C **93**, 024918 (2016).
- [14] D. K. Mishra, P. Garg, P. K. Netrakanti and A. K. Mohanty, Phys. Rev. C **94**, 014905 (2016).
- [15] D. K. Mishra, P. Garg, P. K. Netrakanti and A. K. Mohanty, J. Phys. G **42**, 105105 (2015).
- [16] P. Garg, D. K. Mishra, P. K. Netrakanti, B. Mohanty, A. K. Mohanty, B. K. Singh and N. Xu, Phys. Lett. B **726**, 691 (2013).
- [17] P. Garg, D. K. Mishra, P. K. Netrakanti, A. K. Mohanty and B. Mohanty, J. Phys. G **40**, 055103 (2013).
- [18] P. Garg, D. K. Mishra, P. K. Netrakanti and A. K. Mohanty, Eur. Phys. J. A **52**, 27 (2016).
- [19] S. Q. Feng and Y. Zhong, Phys. Rev. C **83**, 034908 (2011).
- [20] I. G. Bearden *et al.* [BRAHMS Collaboration], Phys. Rev. Lett. **93**, 102301 (2004).
- [21] F. Videbaek, J. Phys. Conf. Ser. **50**, 134 (2006).
- [22] F. C. Zhou, Z. B. Yin and D. C. Zhou, Chin. Phys. Lett. **27**, 052503 (2010).
- [23] S. Li and S. Q. Feng, Chin. Phys. C **36**, 136 (2012).
- [24] I. C. Arsene *et al.* [BRAHMS Collaboration], Phys. Lett. B **677**, 267 (2009).
- [25] L. Ahle *et al.* [E802 Collaboration], Phys. Rev. C **60**, 064901 (1999).
- [26] J. Barrette *et al.* [E877 Collaboration], Phys. Rev. C **62**, 024901 (2000).
- [27] B. B. Back *et al.* [E917 Collaboration], Phys. Rev. Lett. **86**, 1970 (2001).
- [28] J. Stachel, Nucl. Phys. A **654**, C119 (1999).
- [29] D. Thakur, S. Tripathy, P. Garg, R. Sahoo and J. Cleymans, arXiv:1601.05223 [hep-ph], To appear in Adv. in High. Eng. Physics (2016).
- [30] R. Picha, PhD Thesis, University of California, Davis, USA, 2005, UMI-31-82520.
- [31] B. I. Abelev *et al.* [STAR Collaboration], Phys. Lett. B **655**, 104 (2007).
- [32] B. I. Abelev *et al.* [STAR Collaboration], Phys. Rev. Lett. **97**, 152301 (2006).
- [33] B. I. Abelev *et al.* [STAR Collaboration], Phys. Rev. C **75**, 064901 (2007).
- [34] Cumulants of proton and anti-proton distribution measured by STAR experiment.
- [35] B. I. Abelev *et al.* [STAR Collaboration], Phys. Rev. C **81**, 024911 (2010).